THREE-COLOUR PHOTOMETRY OF GH PEGASI

R. K. SRIVASTAVA and T. D. PADALIA
Uttar Pradesh State Observatory, Naini Tal, India

(Received 9 January, 1974)

Abstract. The geometrical elements of the system GH Pegasi and a slightly improved period of $2^d.556136$ have been given.

1. Introduction

The eclipsing binary GH Pegasi (=BD +14°4684=HD 207741) was discovered by Strohmeier and Knigge (1960a, 1960b). The system was observed by Filatov (1961) and a photographic light curve was given by Strohmeier (1962). No details about the orbital elements are available in the literature.

2. Observations

The star was observed photoelectrically on the 38-cm reflector of Uttar Pradesh State Observatory, using an unrefrigerated 1P21 photomultiplier, the conventional *U*, *B* and *V* filters of Johnson and Morgan (1953) and standard d.c. techniques. A total of 18 nights of observations have been obtained during the period October – December, 1972.

All the reductions were done using BD +14°4685 as the comparison star. The particulars of the stars are given in Table I.

TABLE I

Particulars of variable and comparison stars

Star	α_{1855}	δ_{1855}	M_v	S_p
GH Pegasi = BD +14°4684	$21^h43^m54^s.6$	+14°34′.1	$8^m.8$	K
Comparison Star = BD +14°4685	$21^h44^m25^s.6$	+14°37′.1	$8^m.8$	B

The average standard deviations of the comparison star on 11 nights are $0^m.024$, $0^m.015$ and $0^m.015$ in *U*, *B* and *V* filters respectively.

Ten standard stars taken from the list of Johnson and Morgan (1953) have been observed to reduce the data to the standard system.

3. Epoch and Period

The following primary and secondary minima have been observed, the times of

Astrophysics and Space Science **29** (1974) 435–438.

minima having been determined through the graphical method, with an accuracy better than $0^d.001$:

Primary Minima, JD (Hel)	Secondary Minima, JD (Hel)
(1)2441603.284 (3)2441621.198	(1)2441630.145
(2)2441616.106 (4)2441639.084	(2)2441653.143

On the basis of the elements given by Strohmeier (1962), viz., Primary Minimum $=$JD 2426647.345$+2^d.556138$E, the primary minimum was found shifted in phase by $-0^d.007$. On this basis, a slightly improved systemic period of $2^d.556136$ has been obtained.

4. Light Curves and Elements

The results in U, B and V colours are presented. The primary minimum has depths of $0^m.620$, $0^m.610$ and $0^m.476$ (as read from the computed light curve) in U, B and V filters respectively, while the secondary minimum has the depths of $0^m.177$, $0^m.102$ and $0^m.127$ in these respective filters. The χ-values, given in Table II (b), indicate that the primary eclipse is a transit while the secondary eclipse is an occultation. The solution is derived on the basis of darkened discs and a value of the limb darkening $x=0.6$ is chosen for both the eclipses. The nomograph for $x=0.6$ indicates that the eclipse is partial. How-

TABLE II

In this table the subscripts 1 and 2 refer respectively to the greater (brighter) and smaller (fainter) component

(a) Light elements of GH Pegasi

$x=0.6$ (assumed)	$\alpha_0{}^{oc}=0.53$
$P=2^d.556136$	$\alpha_0{}^{tr}=0.61$
$k=0.90$	

(b) Geometrical elements of GH Pegasi

Elements	U filter	B filter	V filter	Mean of the U, B and V filters
$1-\lambda_1$	0.435	0.430	0.355	
$1-\lambda_2$	0.150	0.090	0.110	
L_1	0.747	0.827	0.766	
L_2	0.253	0.173	0.234	
i	84°.0	82°.5	81°.4	82°.6
r_1	0.178	0.192	0.194	0.188
r_2	0.160	0.173	0.175	0.169
J_1/J_2	2.900	4.778	3.227	3.635
θ_e	18°.9	20°.2	20°.0	19°.7
χ^{pr}	0.321	0.327	0.332	
χ^{sec}	0.419	0.411	0.390	

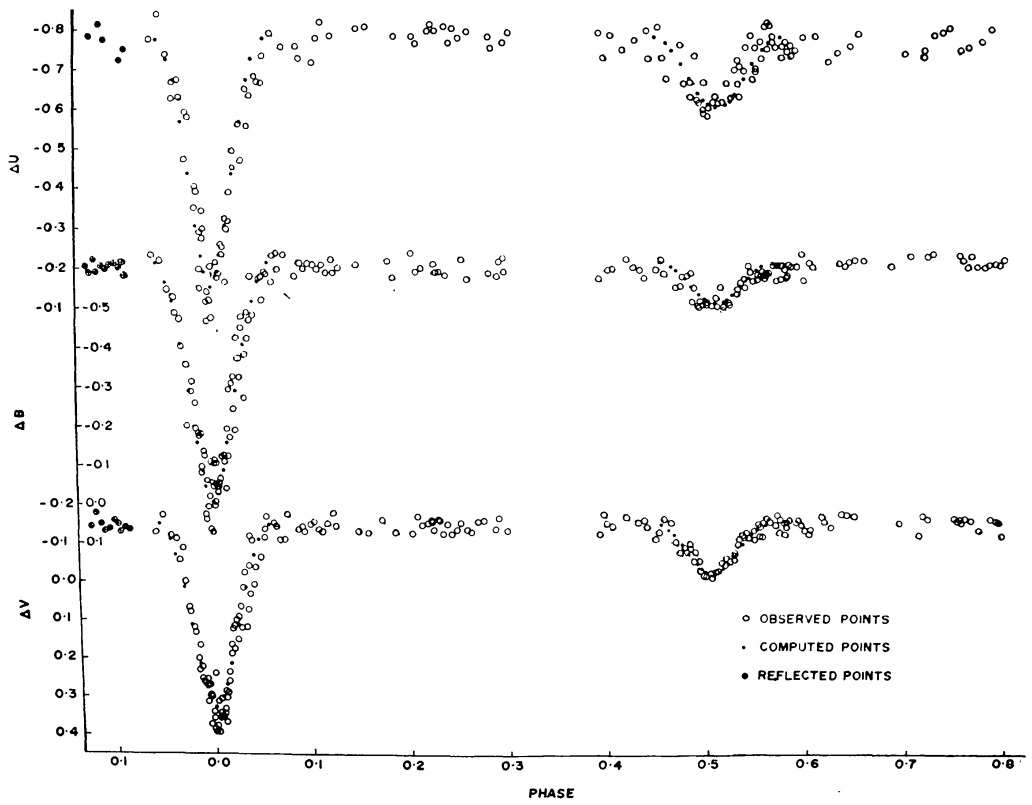

Fig. 1. Light curves of GH Pegasi

ever, two solutions assuming the eclipse to be respectively partial or total have been tried. It was found that the assumption of total eclipse does not lead to a satisfactory solution. Hence the elements have been derived assuming the eclipse to be partial The value of $k=0.90$ has been obtained after several trials. The elements have been derived with the help of Merrill's (1950) tables of χ-function. It is important to mention that the depth of secondary minimum is not reliable due to its shallowness. Hence all the derivations are based on the information derived from the primary minimum. The geometrical elements are listed in Table II. Apparently there seems no necessity for rectification.

The computed points are determined from the well known χ-relation, and are plotted as filled circles in Figure 1. A few observations outside of primary minimum and around phase 0.1 have been reflected around phase 0.9 and these are plotted in Figure 1 as crosses inside open circles.

Acknowledgement

We are thankful to Dr S. D. Sinvhal for suggesting the problem and for helpful discussions.

References

Filatov, G. S.: 1961, *Astronom. Circ.*, No. 223.
Johnson, H. L. and Morgan, W. W.: 1953, *Astrophys. J.* **117**, 339.
Merrill, J. E.: 1950, *Princeton Contr.*, No. 23.
Strohmeier, W. and Knigge, R.: 1960a, *Kleine Veröffentl. Remeis-Sternw. (Bamberg)*, No. 5.
Strohmeier, W. and Knigge, R.: 1960b, *Kleine Veröffentl. Remeis-Sternw. (Bamberg)*, No. 8.
Strohmeier, W.: 1962, *Inf. Bull. Variable Stars.*, No. 9.

ABSTRACTS OF FORTHCOMING PAPERS

J. D. Mihalov: **Distant Bow Shock Observations by Explorer 33.** (Received 25 January; in revised form 8 February, 1974.)

Locations, orientations and magnetic field changes are given for 135 bow shock crossings at distances downstream from Earth between 84 and 117 Earth radii. The shock locations bracket locations calculated for the hypersonic analogue by Dryer and Heckman for a Mach number of 3.8. The shock normal vectors have been calculated using magnetic coplanarity. The average normal vectors have a greater inclination by $\sim 17 \pm 5$ deg from the symmetry axis than the Dryer and Heckman shock orientations for a 3.8 Mach number. Over a range of downstream distances from 60 to 115 Earth radii, the median magnetic field magnitude jump across the shock changes from 1.90 to 1.70 times.

Noel Cary: **Main-Sequence Models for Massive Zero-Metal Stars.** (Received 13 November; in revised form 15 February, 1974.)

Zero-age main-sequence models for stars of 20, 10, 5, and 2 $M_\odot$ with no heavy elements are constructed for three different possible primordial helium abundances: $Y = 0.00$, $Y = 0.23$, and $Y = 0.30$. The latter two values of Y bracket the range of primordial helium abundances cited by Wagoner. With the exceptions of the two 20 $M_\odot$ models that contain helium, these models are found to be self-consistent in the sense that the formation of carbon through the triple-alpha process during pre-main sequence contraction is not sufficient to bring the CN cycle into competition with the proton-proton chain on the ZAMS. The zero-metal models of the present study have higher surface and central temperatures, higher central densities, smaller radii, and smaller convective cores than do the Population I models with the same masses. If galaxies containing the zero-metal stars were formed as recently as one third the Hubble time, they would likely appear very blue today – perhaps bluer even than most known quasars – and their redshifted effective temperatures could range as high as 3×10^4 K to 4×10^4 K.

G. Cavallo and A. Messina: **On the Initial Energy of Supernova Remnants.** (Received 4 March, 1974.)

An examination of the histogram of the Supernova Remnants radii allows one to deduce: (1) some support for the existence of a fairly dense galactic halo at least up to a few kpc from the galactic plane; (2) a first approximation for the initial energy distribution. Although the precise shape is still in doubt and various possibilities exist, one can conclude that the supernova rate should be no less than 1/150 SN yr^{-1}, and no more than 1/170 SN yr^{-1}; the average initial energy should be larger than 1.4×10^{49} erg.

L. H. Aller and C. D. Keyes: **Spectral Line Changes in RR Telescopii, 1961–72.** (Received 5 March, 1974.)

Spectrophotometric measurements of the nova-like variable RR Tel secured at Cerro Tololo in 1972 with a photoelectric spectrum scanner are compared with previously reported photographic measurements and some photoelectric spectrum scans obtained at Mt. Stromlo in 1961. We have attempted to use these data to calibrate the photographic measurements which had much higher spectral resolution. This effort is complicated by the change of the spectrum with time; [Fe VII] and [Ne V] seem to be increasing with respect to Hβ, while [Fe VI], [O III], and [Ne III] appear to be weakening.

M. Clutton-Brock: **Why Is The Universe Homogeneous?** (Received 5 March, 1974.)

The very early universe must have been extremely homogeneous, even on scales far exceeding the particle horizon. Within the framework of the standard Friedmann cosmology, homogenization can only be achieved by quantum effects which violate classical causality. This could happen when the particle horizon was smaller than the Compton wavelength of the pion. The assumption that statistical departures from equilibrium started to grow after this epoch leads to a prediction of the density fluctuations at recombination. The amplitude ν of the fluctuations should have a maximum of about 0.007 on scales of $8_{10}17\ M$. For smaller scales, $\nu \propto M^{+1/6}$, and for larger scales, $\nu \propto M^{-1/2}$. This suggests that superclusters condense out at a red shift of about 11, and clusters and then galaxies form shortly after by fragmentation.

P. G. Kazantzis and C. L. Goudas: **Application of Higher Order Variations of Motion.** (Received 14 March, 1974.)

The theoretical considerations developed in a previous paper are applied with the aid of the CDC-3300 computer and examples of new families of doubly symmetric solutions of the restricted three-dimensional problem obtained thereof are presented. Rough estimates of initial conditions of these families have been obtained by applying an extension of the scanning technique developed by Hénon (1966).

Wolfgang Kundt: **Dragfree Spaceprobe.** (Received 14 March, 1974.)

Dragfree missions are needed for very accurate planetary sounding, and for testing of Einstein's theory of gravity. With the state-of-the-art technology, drag compensation in the approximate plane of a spaceprobe orbit is feasible down to $10^{-13}g$, ($g = 10^3$ cm s^{-2}); for the out-of-plane component, the achievable dragfree level is only $10^{-12}g$. However, future technology (larger launchers, electric propulsion) can decrease these limits.

A. Peton: **Étude du système AX Mon.** (Reçu le 15 mars, 1974.)

Nous avons divisé cette étude en 4 parties principales.

Nous montrons dans la première partie l'importance du rôle de l'enveloppe sur la composition et les variations spectrales, l'influence du mouvement orbital sur l'intensité des absorptions d'enveloppe et la décroissance constante de l'étendue de l'enveloppe pendant les 11 ans couverts par nos observations.

L'étude dans la seconde partie de la raie Fe II λ4233 permet de dégager l'influence du mouvement orbital et notamment son action sur la fine absorption d'enveloppe, montre la décroissance de l'étendue de l'enveloppe par l'intermédiaire d'un système de courbes isophases, indique que l'émission est maximum au maximum d'extension de l'enveloppe et que la raie d'émission photosphérique est visible sur tous les cycles au voisinage de la phase 0.500 de la période orbitale.

L'examen des vitesses montre qu'il existe une pulsation des zones émissives liée au mouvement orbital. L'accélération des couches internes change de sens en allant de l'apoastre au périastre, tandis que l'accélération des couches extérieures augmente. Ces mouvements provoquent des changements de densité qui peuvent expliquer les variations d'intensité du spectre métallique de l'enveloppe.

Dans la troisième partie nous examinons le comportement des variations photométriques de AX Mon relativement à trois échelles de temps:

(a) à très court terme ($\leqslant$ 4 h), les variations peuvent être importantes et atteindre 0.1 mag. Elles semblent caractéristiques d'une éjection de matière sous forme de jets gazeux très chauds.

(b) à court terme ($>$ 1 j), les variations peuvent être interprétées comme des variations d'absorption des couches basses de l'enveloppe: elles sont liées à l'intensité des absorptions satellites de la raie Fe II λ4233.

(c) à moyen terme ($>$ 3 ans), nous observons une diminution sensible de l'amplitude des variations du type b, mais aucun changement de la valeur moyenne autour de laquelle s'effectuent les variations.

Cette remarque nous a permis de déterminer les indices de AX Mon ($V = 6{,}77$; $B - V = +0{,}33$; $U - B = -0{,}66$). L'amplitude de ces variations semble d'autant plus grande que l'enveloppe est plus étendue.

Nous montrons dans la dernière partie que le type spectral de l'étoile chaude du système AX Mon peut être estimé à B 0.5 V et celui de l'étoile froide à K 2 II.

Le rapport de masse est estimé en choisissant la courbe de vitesse des raies à caractère α Cygni pour représenter l'étoile B. Ce choix conduit à des résultats en très bon accord avec l'observation.

Dans le modèle qui en résulte, la secondaire remplit entièrement son lobe de Roche et permet des échanges de masse de l'étoile K vers l'étoile B. L'angle i élevé ($i = 79°$) permet une observation quasi-équatoriale et explique pourquoi, malgré la faible excentricité, nous pouvons observer des effets de marée et les changements spectraux qui en résultent.